P
2mil

NASA TECHNICAL NOTE

NASA TN D-7562

NASA TN D-7562

EXPERIMENTAL AND ANALYTICAL DETERMINATION OF VIBRATION CHARACTERISTICS OF CORRUGATED, FLEXIBLY SUPPORTED, HEAT-SHIELD PANELS

by Huey D. Carden

Langley Research Center
Hampton, Va. 23665

NATIONAL AERONAUTICS AND SPACE ADMINISTRATION • WASHINGTON, D. C. • MAY 1974

1. Report No.	2. Government Accession No.	3. Recipient's Catalog No.
NASA TN D-7562		

4. Title and Subtitle	5. Report Date
EXPERIMENTAL AND ANALYTICAL DETERMINATION OF VIBRATION CHARACTERISTICS OF CORRUGATED, FLEXIBLY SUPPORTED, HEAT-SHIELD PANELS	May 1974
	6. Performing Organization Code
7. Author(s)	8. Performing Organization Report No.
Huey D. Carden	L-9364
	10. Work Unit No.
9. Performing Organization Name and Address	502-32-02-04
NASA Langley Research Center Hampton, Va. 23665	11. Contract or Grant No.
	13. Type of Report and Period Covered
12. Sponsoring Agency Name and Address	Technical Note
National Aeronautics and Space Administration Washington, D.C. 20546	14. Sponsoring Agency Code

15. Supplementary Notes

16. Abstract

Experimental and analytical natural frequencies, nodal patterns, and typical modal displacements for a corrugated, flexibly supported, heat-shield panel are discussed. Good correlation was found between the experimental data and NASTRAN analytical results for the corrugated panel over a relatively wide frequency spectrum covered in the investigation. Of the two experimental techniques used for mode shape and displacement measurements (a noncontacting displacement sensor system and a holographic technique using a helium-neon, continuous-wave laser), the holographic technique was found, in the present investigation, to be faster and better suited for determining a large number of complex nodal patterns of the corrugated panel.

17. Key Words (Suggested by Author(s))	18. Distribution Statement
Vibration Heat-shield panels	Unclassified – Unlimited STAR Category 32

19. Security Classif. (of this report)	20. Security Classif. (of this page)	21. No. of Pages	22. Price*
Unclassified	Unclassified	22	$3.00

*For sale by the National Technical Information Service, Springfield, Virginia 22151

EXPERIMENTAL AND ANALYTICAL DETERMINATION OF VIBRATION CHARACTERISTICS OF CORRUGATED, FLEXIBLY SUPPORTED, HEAT-SHIELD PANELS

By Huey D. Carden
Langley Research Center

SUMMARY

Results of an experimental and analytical study of the room-temperature vibration characteristics of a corrugated, flexibly supported, thorium-dispersed nickel-chrome (designated TDNiCr) heat-shield panel are presented.

The capability of the NASTRAN computer program for accurate analysis of the corrugated panel was verified by comparisons between the analytical and the experimental data. Good correlation was indicated between the experimental and analytical natural frequencies, nodal patterns, and typical modal displacements for a relatively wide frequency spectrum.

The experimental natural frequencies, nodal patterns, and modal displacements obtained by using a noncontacting displacement sensor system and a holographic technique indicated that in the present investigation, the holographic technique was faster and better suited for determining the many complex nodal patterns of the corrugated panel.

INTRODUCTION

Substantial efforts have been expended over the past several years in the development of reliable lightweight metallic panels to serve as the thermal insulation system of high-speed vehicles such as the space shuttle and proposed hypersonic aircraft. These efforts have been concerned primarily with structural concepts for design of metallic shields (ref. 1), experimental evaluation of materials for heat-shield applications (ref. 2), and problems of flutter (refs. 3 to 5).

Many panel designs have been proposed as thermal protection systems (TPS). One of the concepts under study is a Langley Research Center design consisting of a multiple-clip-supported, corrugated single-skin heat shield constructed of thorium-dispersed nickel chrome (designated TDNiCr). (See ref. 6.)

Vibration characteristics of candidate panels are important in understanding panel-flutter behavior, load-carrying ability, and fatigue-resistance properties. Thus, as a part

of the evaluation effort, studies were conducted to demonstrate applicability of current analytical and experimental approaches to measure and predict basic vibration characteristics of corrugated, clip-supported panels. (See refs. 7 and 8.)

This paper presents the results of a combined experimental and analytical study of the room-temperature vibration characteristics of a TDNiCr, thin-skin, corrugated heat-shield panel mounted on multiple-clip supports. Experimental data presented include natural frequencies, nodal patterns, and typical modal displacements for the panel which were determined holographically and by a noncontacting displacement sensor. Correlations of the experimental results with the NASTRAN structural analysis computer program are made.

PANEL DESCRIPTION

The panel model, shown in figure 1, is composed of three basic components, the corrugated skin, the support clips, and the insulation (not shown or used in the investigation). The single corrugated skin is fabricated from 0.635 mm TDNiCr (thorium-dispersed nickel-chrome) sheet. Overall panel size is 296.9 mm in width and 558.8 mm in length; corrugations have 91.3 mm pitch and 9.15 mm depth with 23.0 mm flats between corrugations. The panel is bolted to steel channels that are in turn bolted to a metal plate to serve as a platform for vibration testing.

The 12 support clips (see inset figure in fig. 1) are formed from 0.635-mm TDNiCr sheet and are 17.5 mm wide, 76.0 mm long, and have a 6.1- by 60.5-mm slot cut out of the leg of the clip. The supports are joined to the panel with machine screws at dimpled sections on the flats between the corrugations. The support clips carry the normal panel loads into the primary structure. The clips in the center row of supports are rotated 90° to the others.

INSTRUMENTATION AND TEST PROCEDURE

Panel Excitation

A 6.7-N electrodynamic shaker shown in figure 2 was used to induce vibrations of the panel. One of two methods was used to attach the shaker to the panel depending upon the method used to measure motions of the panel. In figure 2(a) a small, stiff lightweight attachment wire is shown glued to the panel. This attachment allows appreciable (but less than 6.7 N) input forces to act on the panel during modal surveys with the noncontacting proximity sensor system described in this section. Shown in figure 2(b) is a soft, flexible lightweight attachment wire clamped to the panel edge with a screw and nut to satisfy the extremely small input force requirements for the holographic system also described in

this section. In each of the test series a vibration exciter control was used to drive the power amplifier of the shaker.

Deflection Measurement

Two systems were employed for measuring panel deflections for nodal pattern determination. Limited use was made of the first system, a noncontacting proximity-sensor system, described fully in reference 9, for measuring out-of-plane deflections at resonance. Resonance was established by use of the shaker and by observing on an oscilloscope the Lissajous figure resulting from the input and response signals. Resonance was maintained, and the mobile unit shown in figure 3(a) was used for a survey of the displacements; thus, the nodal patterns over the entire panel surface are defined. The displacement and phase relative to the force was automatically plotted using an x,y plotter.

In the second system, shown in figure 3(b), a holographic technique using a helium-neon, continuous-wave laser was employed for deflection and nodal pattern determination. With the holographic method, only very small displacements are necessary and the nodal pattern of the entire panel surface can be obtained at one time. The system does require, however, an isolated table (granite block in fig. 3(b)) to avoid background noise and vibrations. Details of the holographic technique and some of the related theory are discussed more fully in reference 10. In the method a photographic plate exposure is made of the nonvibrating panel. The exposed photographic plate, which is called a hologram, is developed and carefully replaced in the photographic plate holder where it was originally held. When the hologram is illuminated with the laser light, an image of the panel is superimposed on the actual panel. If the panel vibrates, light from the deformed panel interacts with the stored image of the nonvibrating panel (produced by the hologram) and moving interference fringe patterns form. When the exciter control of the shaker is slowly tuned, the fringe pattern appears to be stationary when the panel vibrates sinusoidally in a normal mode. The frequencies of the stationary patterns are noted during a sweep through the frequency range of interest. A time-averaged hologram (time-exposure) of each of the panel nodal patterns is then made at the frequencies previously noted. A 35-mm camera positioned behind the time-averaged hologram was used to photograph the fringe patterns presented herein.

ANALYSIS AND PANEL IDEALIZATION

The NASA finite element structural analysis computer program (NASTRAN) was used to compute natural frequencies and nodal patterns of the panel for comparison with experimental data. This program is documented in references 11, 12, and 13.

Figure 4(a) illustrates the idealization involved in applying the NASTRAN computer program to the corrugated panel. To avoid splitting the clips in the center row of supports, advantage of only one plane of symmetry of the panel was used in the modeling. Appropriate symmetric and antisymmetric constraints were applied to the center line of the panel to obtain all the modes of the panel. Quadrilateral plate elements from the NASTRAN element library were used.

As indicated in figure 4(b) the corrugations were modeled approximately to shape with four elements so that the bending stiffness of the quadrilateral element configuration, calculated on the basis of the area moment of inertia of a typical corrugation, was about 96 percent of the actual panel configuration stiffness. The four-element configuration was chosen since a finer mesh of elements would increase substantially the total degrees of freedom of the panel model for only a slightly better stiffness representation.

To limit further the degrees of freedom in the analysis, a special treatment was used in the region of the supports. It was assumed that the mass of the clips could be neglected and their behavior determined statically from the loads applied to them by the corrugated skin. Consequently, a static analysis was made of a very detailed model (approximately 1900 degrees of freedom) of the clip, as shown at the right of figure 4(a), to obtain a static influence coefficient matrix for the clip. The general element (GENEL) capability of NASTRAN was used to input the influence coefficients of the support clips to represent the supports in the dynamic analysis of the panel.

The element mesh used to model the panel surface, as illustrated in the figure, for the eigenvalue problem resulted in a model with about 1200 degrees of freedom. A standard Guyan reduction procedure was applied to reduce the size to 264 degrees of freedom for the antisymmetric case and 220 degrees of freedom for the symmetric case. Table I presents some of the computational times, number of natural frequencies and mode shapes extracted, and problem size for the panel analyses in level 12 of NASTRAN on a Control Data 6600 computer. An improved version of NASTRAN, Level 15, reduces appreciably the computer solution times shown in table I (ref. 14).

TABLE I.- SUMMARY OF NASTRAN PANEL MODEL AND COMPUTER RESULTS

[Level 12 of NASTRAN]

Structural component	Number of grid points	Number of NASTRAN elements				Degrees of freedom					Computer solution time, min			Output results		
						Static	Dynamic				Static	Dynamic			Dynamic	
							Symmetrical case		Antisymmetrical case							
		CQUAD2	CTRIA2	GENEL	Total elements	After constraints	After constraints	After Guyan reduction	After constraints	After Guyan reduction		Symmetrical case	Antisymmetrical case	Static	Symmetrical case	Antisymmetrical case
Clip support	306	216	36	---	252	1689	----	---	----	---	14	---	---	20 × 20 influence coefficient matrix	----------	----------
1/2 panel	198	162	---	6	168	----	1100	220	1100	264	---	90	120	----------	220 frequencies; 25 modes	264 frequencies; 25 modes

RESULTS AND DISCUSSION

Results of an experimental and analytical study of the room temperature vibration characteristics of the panel are presented in figures 5 to 8. Included in the results are experimental and analytical panel natural frequencies and nodal patterns. A comparison is presented between the nodal patterns determined by use of the NASTRAN computer program and those measured by use of holographic techniques and a noncontacting displacement-sensor system. Also included is a comparison of experimental and analytical displacements for selected panel resonant frequencies.

Panel Natural Frequencies

Measured and computed frequencies as a function of the mode number for the TDNiCr panel are shown in figure 5. Several important points may be deduced from the computed results. First, extremely close spacing of frequencies of the panel is evident. As may be seen from figure 5, 45 computed modes occur below 800 Hz. Second, there are also regions or plateaus where many modes occur with only slight frequency differences. For instance, between the 16th and the 27th modes, the frequency spread of the 12 modes is only 75 Hz. Such density of modes often gives rise to difficulty in experimental identification since coupled nodal patterns usually result. Third, the large jumps or steps in frequency between the plateaus or frequency groups are associated with the number of node lines occurring across the panel width. As examples, the steps in frequency between the 28th and 29th as well as the 43rd and 44th modes resulted when two additional node lines (from 5 to 7 nodes in the former and 7 to 9 nodes in the latter) or a full wavelength in the deflection patterns occurred in the panel-width direction.

Experimental frequencies also are shown in figure 5, and the comparison between the calculations and experiment is good below about the 40th mode. There is excellent correlation between the measured and computed frequencies for the three lowest frequencies which are the lengthwise, sidewise, and torsional rigid-body modes, respectively, of the panel on the support clips. This correlation indicates that the stiffness of the clips was accurately modeled by the static influence coefficients approach. Indeed for the frequencies of the panel through the 14th mode, the agreement in frequency is within 3 percent. For the three highest experimental frequencies shown (the 29th, 36th, and 40th modes), the error is only 10 to 15 percent between the calculated and experimental values. The larger error at these high mode numbers is attributed to the coarseness of the grid mesh of the analytical model used as compared with the close nodal pattern spacing of the panel.

Because of the high modal density of the panel, no attempt was made to search for all possible experimental frequencies, for instance, by moving the shaker attachment point.

The experimental frequencies show, however, that good agreement with the NASTRAN results was achieved over a wide frequency spectrum of the panel.

Panel Nodal Patterns

Measured and computed nodal patterns for eight selected modes of the panel are compared in figure 6. In the figure, sketches of the analytical nodal patterns are compared side by side with photographs of the experimental nodal patterns obtained by the holographic technique. In the sketches, the dashed lines indicate nodal lines whereas in the photographs the broader white lines are node lines for the 4th, 6th, 9th, 10th, 18th, 29th, 36th, and 40th modes of the panel, respectively.

The nodal-pattern comparison in figure 6 indicates good agreement in both the shape and location of the nodal lines between the experimental results and those predicted by the NASTRAN analysis. The data show that the nodes are somewhat regular and many are similar to classical flat-plate nodal patterns. However, because of the occurrence of the localized nodes in the regions of the support clips, especially for the supports at the panel edges, no classification by number of node lines was attempted here.

The experimental nodal patterns of figure 6 are fairly distinct with the exception of figures 6(b) and 6(h) which are relatively poor quality, because of insufficient shaker input force to produce sharp nodes generally noted in the other parts of figure 6. There are also other expected local differences between the experimental and analytical nodal patterns. For instance, in figure 6(a) the node lines along the panel edges trail off on either side of the supports, whereas the analytical nodes extend the full length of the panel edges. In figures 6(b), 6(c), and 6(h), nodes across the panel tend to meander as compared with the straight lines of the analytical nodal patterns. Also in figure 6(e) the experimental nodes on the outer area of the panel did not close into the elliptical patterns as indicated in the analytical counterpart, but the nodes connected into the center node running down the middle corrugation and trailed off to the ends of the panel.

The types of variations noted above are anticipated because of such factors as imperfections and variations in the cross section of the corrugations resulting during fabrication, and differences in the dimples on the flats as well as possible stiffness variations among the support clips. Such influences can all lead to nodal patterns that deviate from those predicted with a geometrically ideal analytical model.

The data in figure 6 also indicate that the holographic technique using the helium-neon, continuous-wave laser is well suited and a powerful experimental tool for determining complex nodal patterns of the corrugated TDNiCr panel. It may be concluded that the idealization of the corrugated panel with a series of quadrilateral elements gives nodal patterns that correlate well with experimental patterns over a wide range of fairly complex panel modes.

All experimental nodal pattern data heretofore presented were obtained by use of a holographic technique. In addition, limited use was made of a noncontacting proximity sensor for nodal pattern determination. In figure 7 is a comparison between a few nodal patterns measured with the noncontacting system and the holographic technique. For completeness, the analytical patterns were also presented.

The data of figure 7 indicate that, in general, the nodal patterns determined with the noncontacting proximity sensor system are identical to those determined with the holographic technique. However, in figure 7(b) the patterns show some differences and illustrate one of the difficulties encountered in this investigation with the noncontacting sensor system. The difficulty is that larger input forces are required to produce measurable panel motion. With the excitation system required for the larger input forces, there was a tendency for the nodal patterns to become distorted. For example, the center node line of figure 7(b) curved to the right away from the shaker location. As a result, only limited use was made of the noncontacting sensor system and most of the experimental nodal pattern data were obtained with the holographic technique.

Panel Modal Displacements

In addition to the frequency and nodal pattern comparisons between experiment and analysis shown in the previous figures, comparisons were also made between the experimental modal amplitudes and the analytical free vibration modal amplitudes. The comparison in figure 8 shows modal amplitude for a representative low, intermediate, and a high mode number (parts (a), (b), and (c) of fig. 8, respectively).

In figure 8 the experimental data are the solid circles, and the analytical data from the NASTRAN analysis are the open circles. Experimental points, normalized for best fit, were determined from an interpretation of the fringe patterns of the holograms by use of the analysis discussed in reference 15. Details of the procedure are not included here but as indicated in reference 15, it is possible to relate the order of the fringes on the hologram to panel displacements.

The displacements in figure 8 indicate that good correlation in the spatial distribution was obtained between the experiment and the NASTRAN analysis. The data further demonstrate the applicability of the holographic approach to measure panel displacements as well as to determine nodal patterns.

The modes in figure 8, as stated above, were chosen to be representative of the full frequency spectrum covered in the investigation. As should be noted in figure 8(c), good modal displacement definition and correlation with experiment was still obtained for the higher panel mode. Even though there are only 16 analytical displacement points across the panel for defining a mode with seven node lines, the analytical model still appears to represent adequately the structural behavior.

CONCLUDING REMARKS

A study was conducted to demonstrate applicability of current analytical and experimental approaches to measure and predict basic vibration characteristics of corrugated, clip-supported panels.

In the study, capabilities for analysis of the corrugated panel were verified by comparisons of the NASTRAN analytical results with experimental natural frequencies, nodal patterns, and modal displacements. Good correlation was found between the experimental and analytical data for the corrugated panel over a relatively wide frequency spectrum.

The good correlation indicated that quadrilateral plate elements in the NASTRAN computer program can be used to model accurately the structural characteristics (stiffness and mass properties) of corrugated panels. Furthermore, the special general element (GENEL) capability in NASTRAN made it possible to represent the many clip supports of the panel by static influence coefficients in the dynamic analysis without increasing the problem size or without loss of accuracy in representing the supports.

Results from this study also indicate that of the two experimental techniques used for mode shape and displacement measurements (a noncontacting displacement sensor system and a holographic technique using a helium-neon, continuous-wave laser), the holographic technique was, in the present investigation, faster and better suited for determining a large number of complex nodal patterns of the corrugated panel.

Langley Research Center,
National Aeronautics and Space Administration,
Hampton, Va., February 15, 1974.

REFERENCES

1. Plank, P. P.; Sakata, I. F.; Davis, G. W.; and Richie, C. C.: Hypersonic Cruise Vehicle Wing Structure Evaluation. NASA CR-1568, 1970.

2. Wichorek, Gregory R.; and Stein, Bland A.: Experimental Investigation of Aluminide-Coated Ta-10W for Heat-Shield Applications. NASA TN D-5524, 1969.

3. Kordes, Eldon E.; Tuovila, Weimer J.; and Guy, Lawrence D.: Flutter Research on Skin Panels. NASA TN D-451, 1960.

4. Weidman, Deene J.: Experimental Flutter Results for Corrugation-Stiffened and Unstiffened Panels. NASA TN D-3301, 1966.

5. Stein, Manuel: Flutter of Panels on Discrete Flexible Supports. NASA TN D-7443, 1974.

6. Stein, Bland A.; Bohon, Herman L.; and Rummler, Donald R.: An Assessment of Radiative Metallic Thermal Protection Systems for Space Shuttle. NASA Space Shuttle Technology Conference – Dynamics and Aeroelasticity; Structures and Materials, NASA TM X-2570, 1972, pp. 267-302.

7. Walton, William C., Jr.; and Naumann, Eugene C.: Panel Vibration and Random Loads. Space Transportation System Technology Symposium, NASA TM X-52876, Vol. II, 1970, pp. 43-57.

8. Carden, Huey D.; Durling, Barbara J.; and Walton, William C., Jr.: Space Shuttle TPS Panel Vibration Studies. NASA Space Shuttle Technology Conference, Vol. III – Dynamics and Aeroelasticity, NASA TM X-2274, 1971, pp. 27-48.

9. Naumann, Eugene C.; and Flagge, Bruce: A Noncontacting Displacement Measuring Technique and Its Application to Current Vibration Testing. Preprint No. 16.18-5-66, Instrum. Soc. Amer., Oct. 1966.

10. Evensen, David A.; and Aprahamian, Robert: Application of Holography to Vibrations, Transient Response, and Wave Propagation. NASA CR-1671, 1970.

11. MacNeal, Richard H., ed.: The NASTRAN Theoretical Manual. NASA SP-221, 1970.

12. McCormick, Caleb W., ed.: The NASTRAN User's Manual. NASA SP-222, 1970.

13. Douglas, Frank J., ed.: The NASTRAN Programmer's Manual. NASA SP-223, 1970.

14. Raney, J. Philip; and Weidman, Deene J.: NASTRAN: A Progress Report. NASTRAN: Users' Experiences. NASA TM X-2637, 1972, pp. 1-11.

15. Powell, Robert L.; and Stetson, Karl A.: Interferometric Vibration Analysis by Wavefront Reconstruction. J. Opt. Soc. Amer., vol. 55, no. 12, Dec. 1965, pp. 1593-1598.

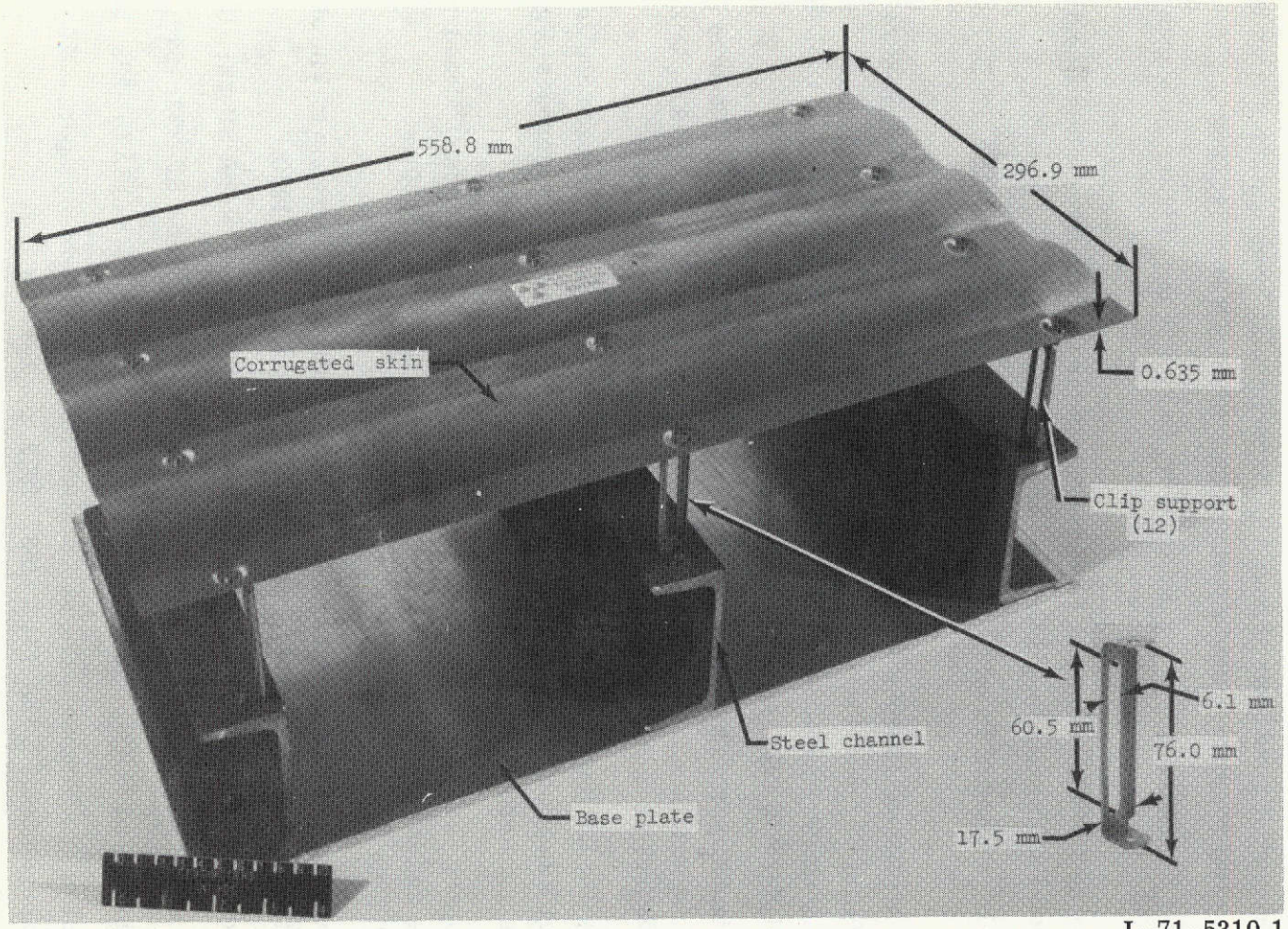

L-71-5310.1

Figure 1.- TDNiCr corrugated single-skin, multiclip-supported heat-shield panel.

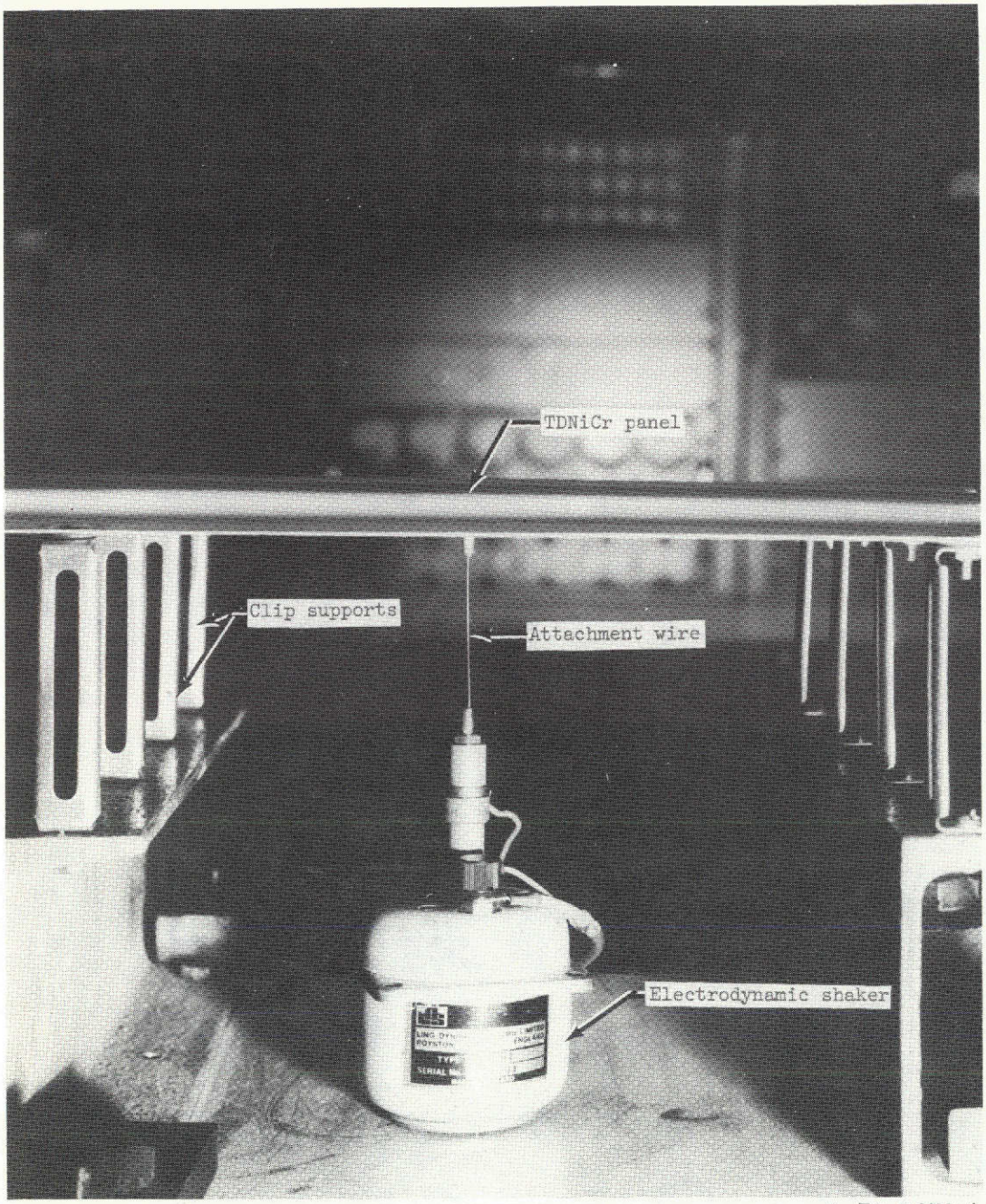

L-73-3670.1

(a) For noncontacting proximity sensor system.

Figure 2.- Panel excitation arrangement.

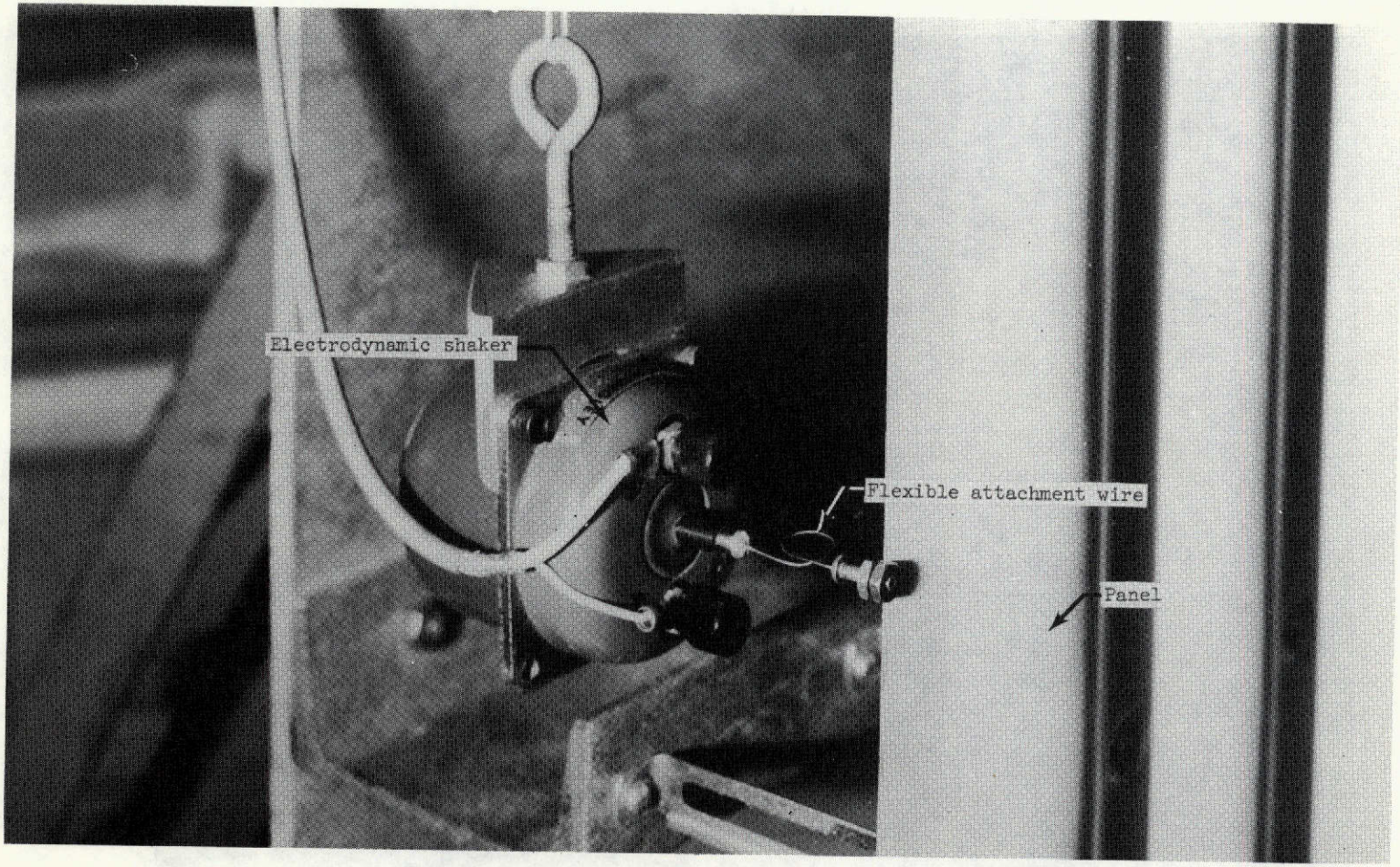

L-73-3671.1

(b) For laser system.

Figure 2.- Concluded.

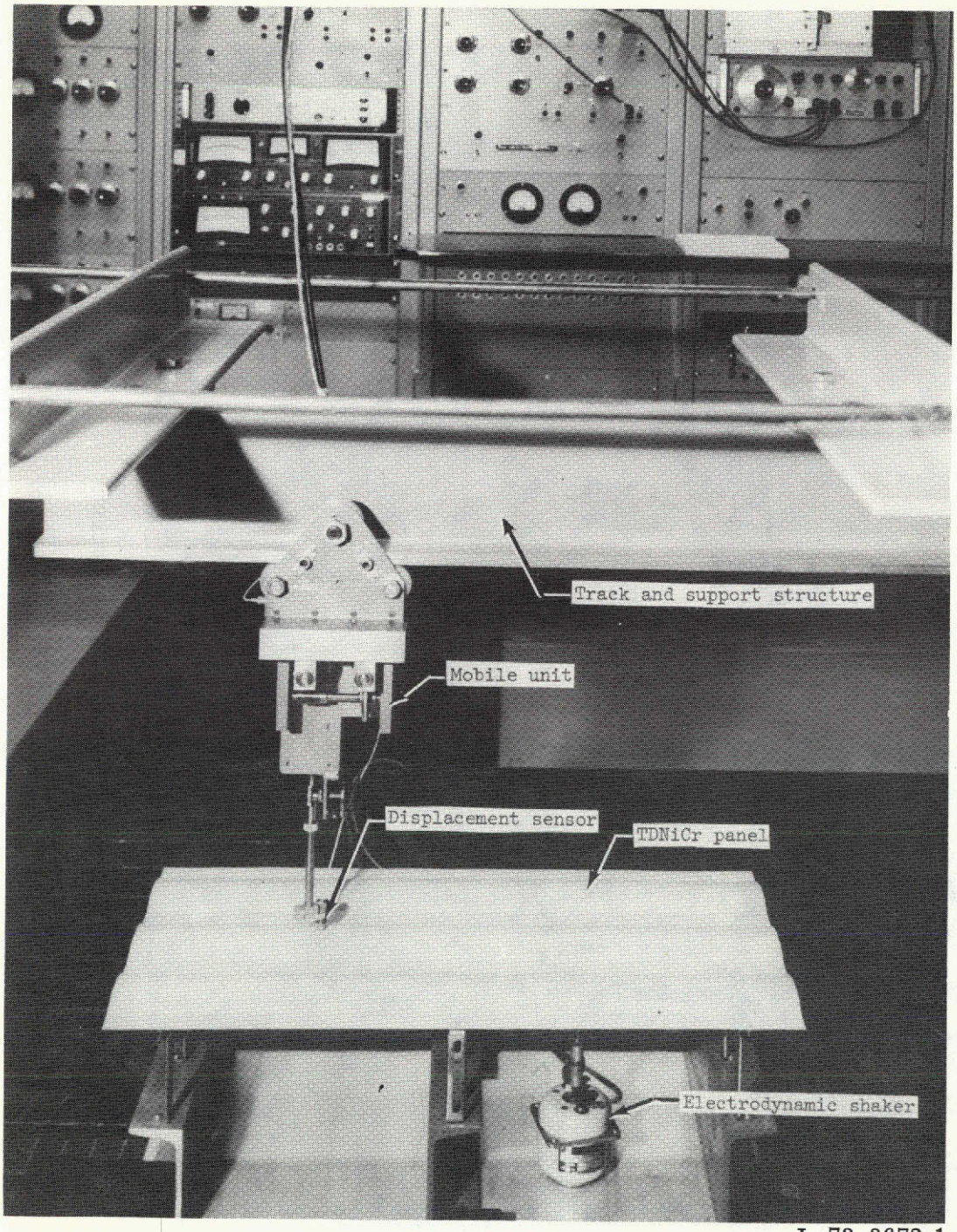

L-73-3672.1

(a) Noncontacting proximity sensor system.

Figure 3.- TDNiCr panel and deflection measurement equipment.

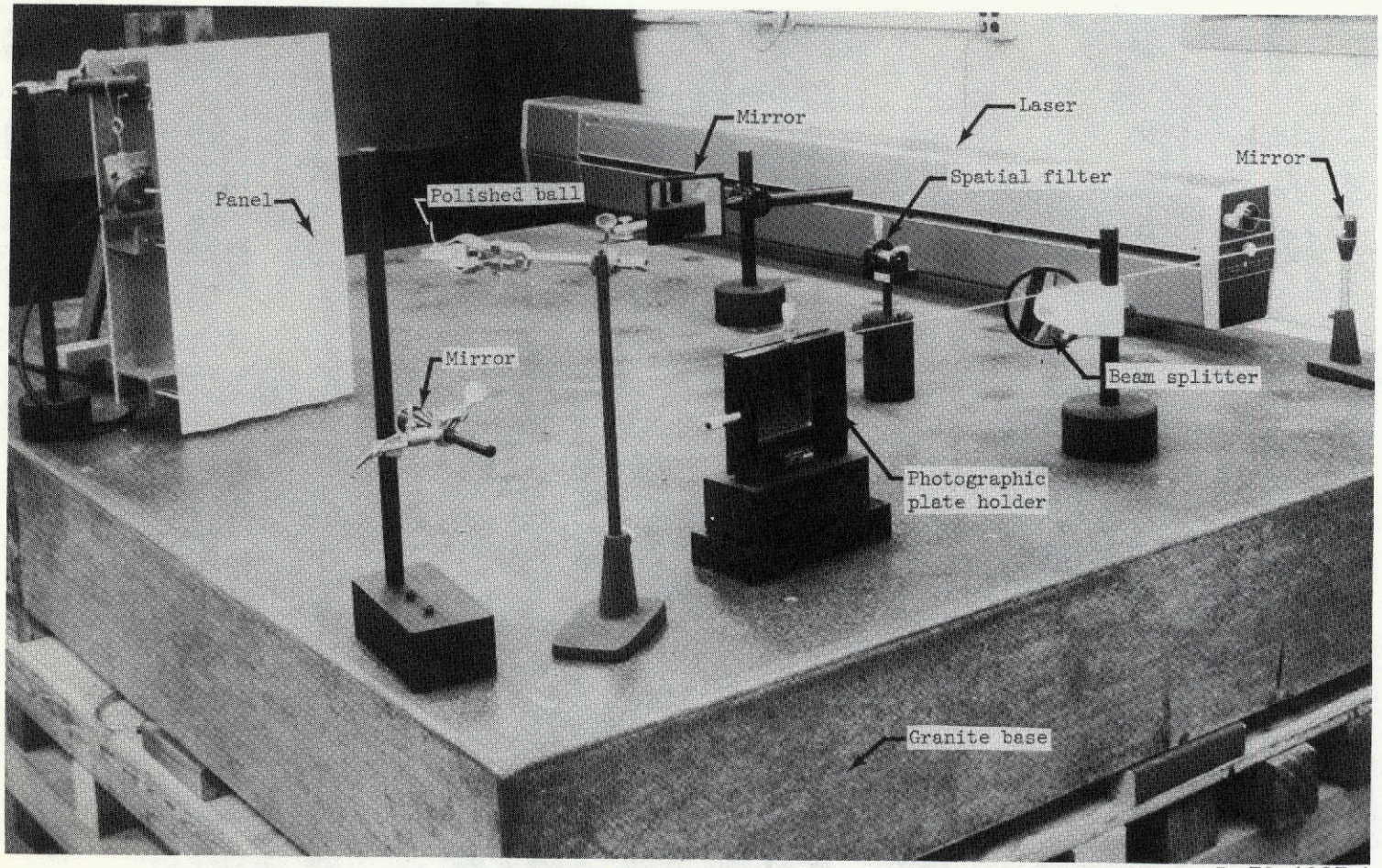

L-73-1987.1

(b) Laser and associated equipment.

Figure 3.- Concluded.

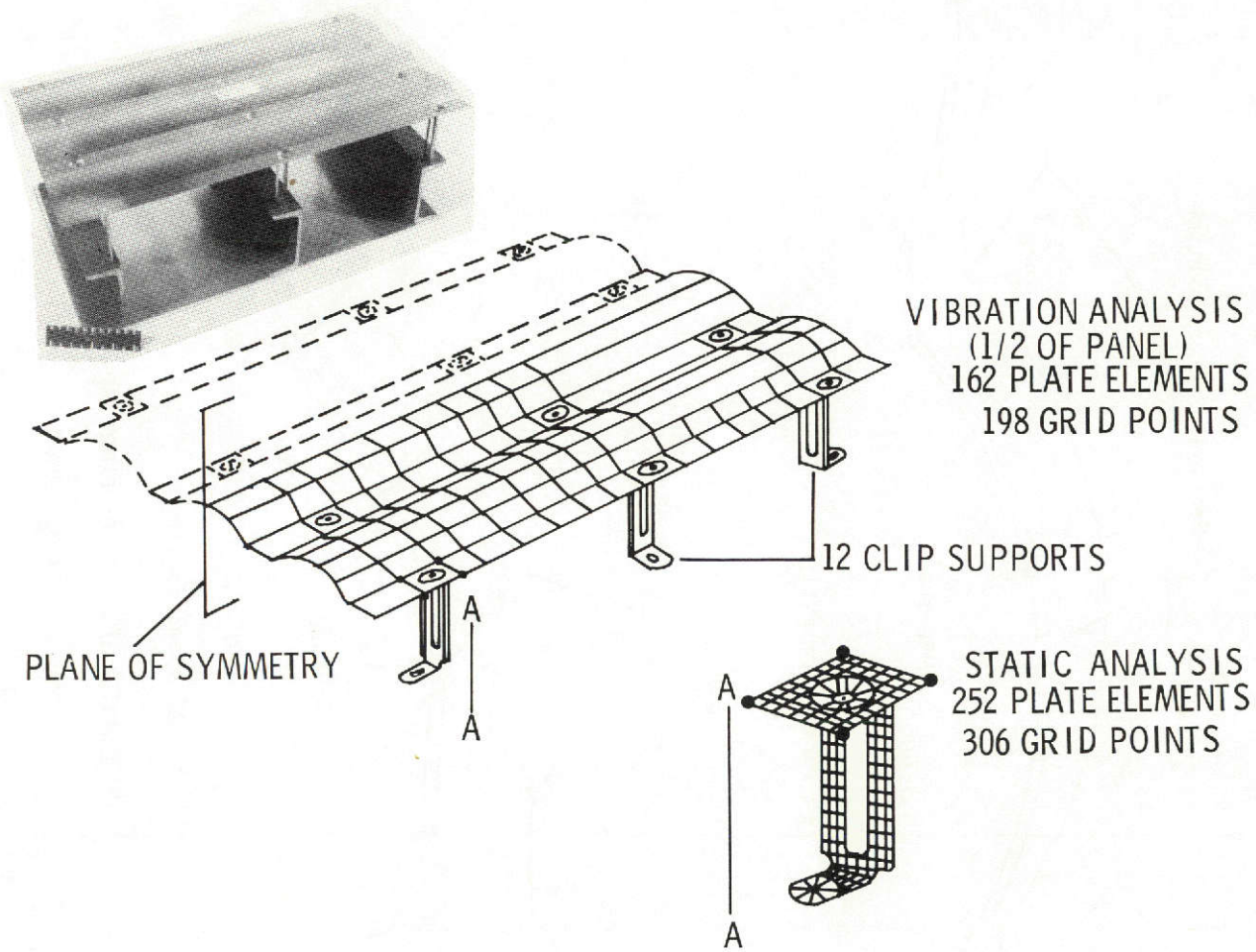

(a) Schematic view of panel.

Figure 4.- Panel and idealization for NASTRAN analysis.

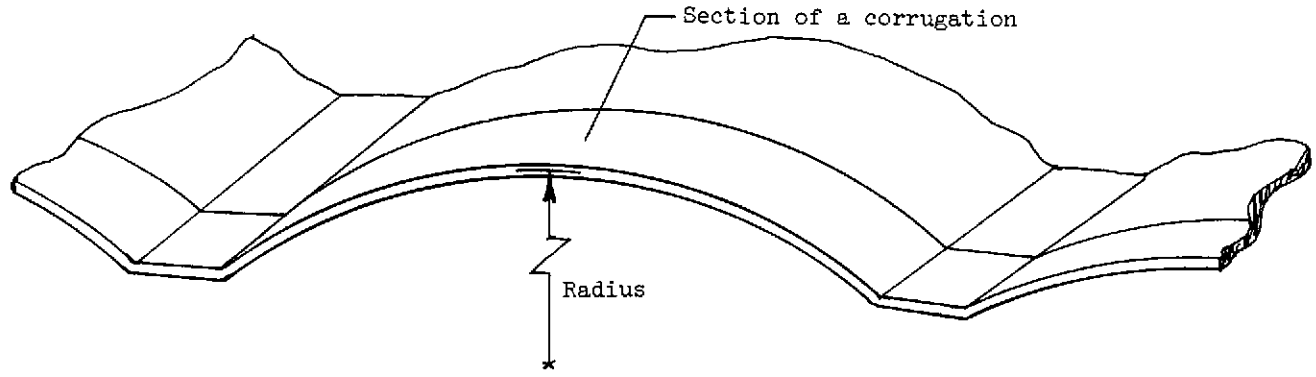

Panel corrugation

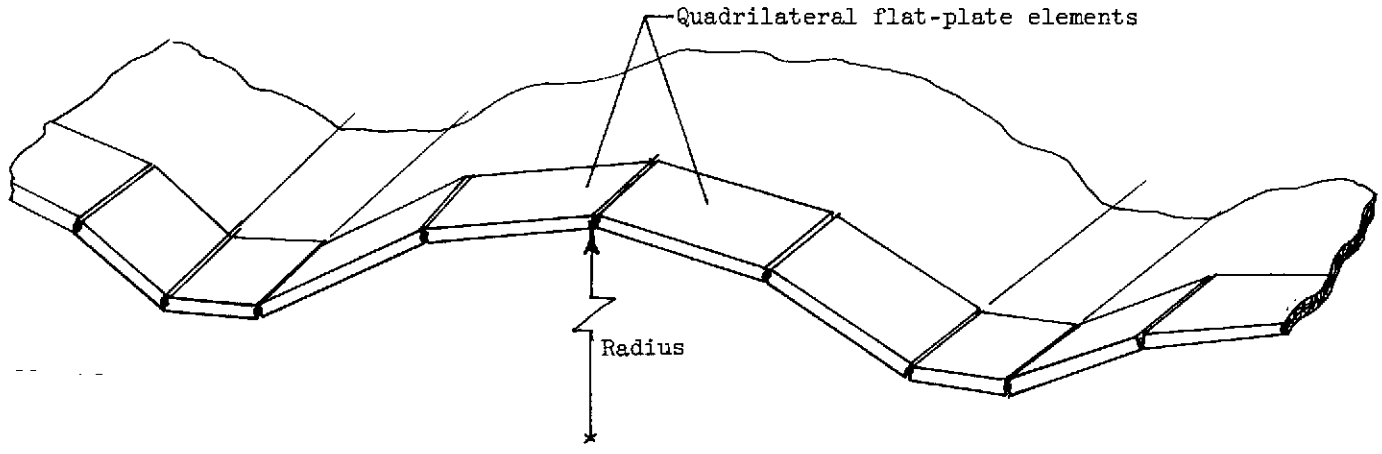

NASTRAN idealization

(b) Details of finite-element model.

Figure 4.- Concluded.

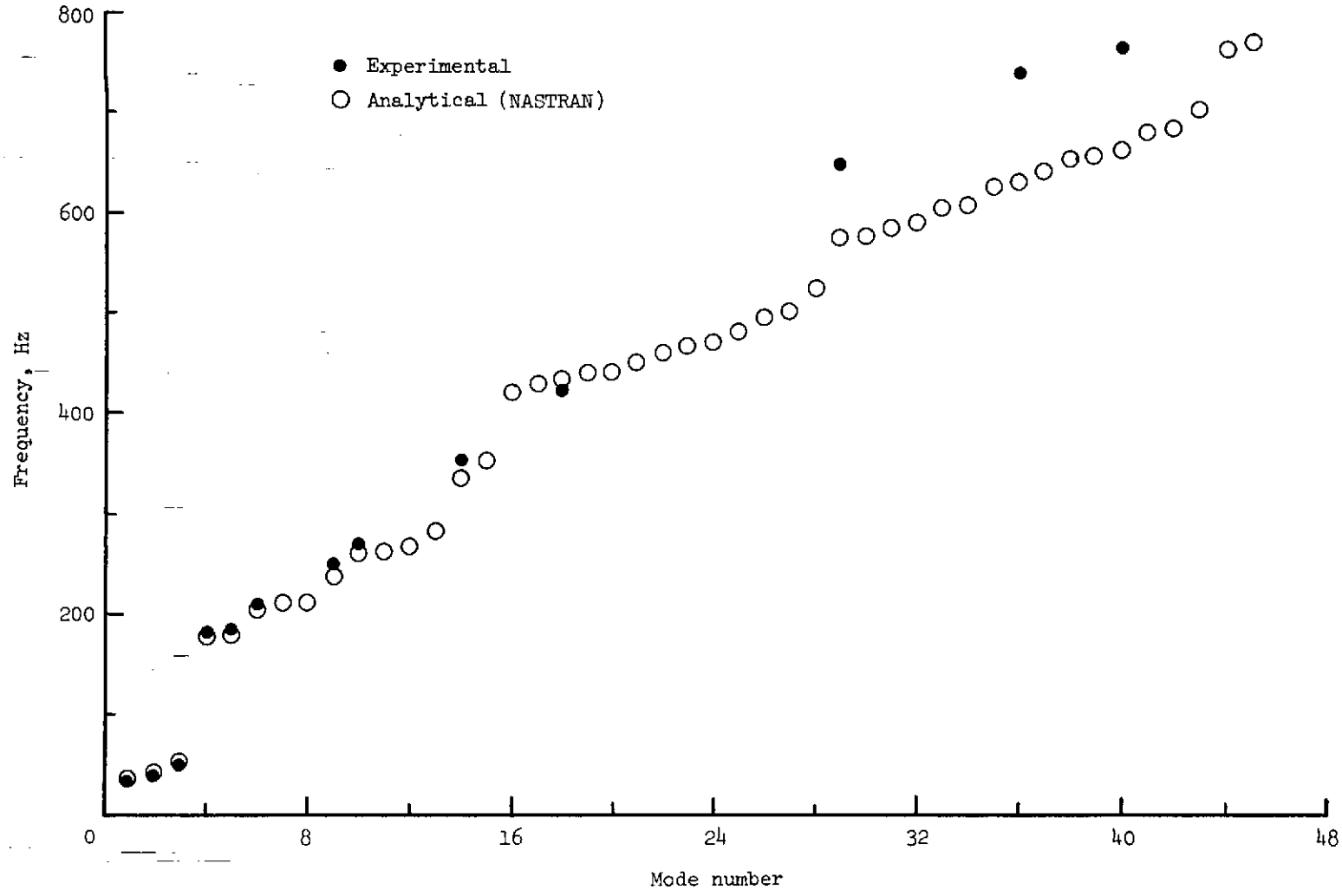

Figure 5.- TDNiCr panel frequencies as a function of mode number.

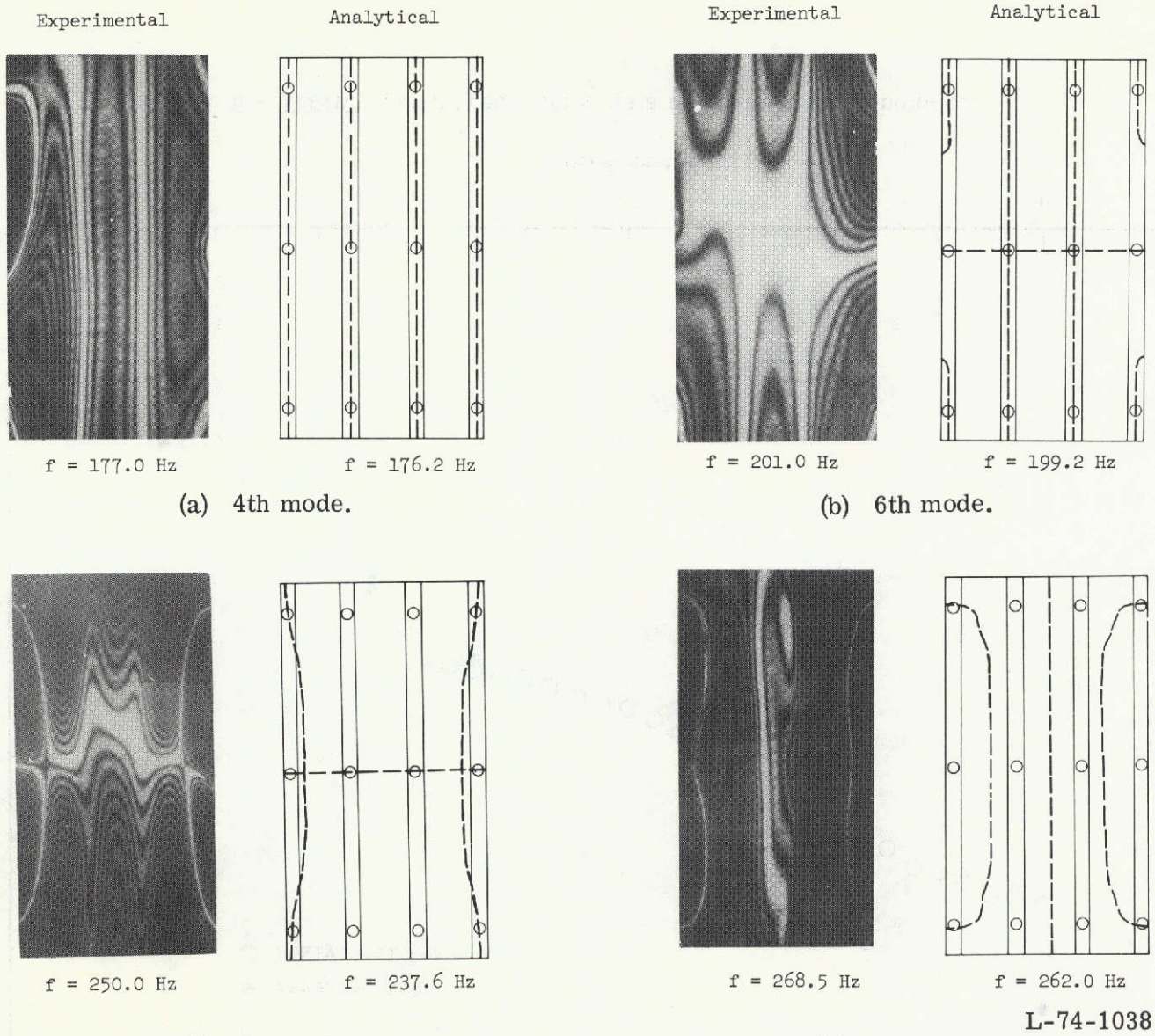

(a) 4th mode.

(b) 6th mode.

(c) 9th mode.

(d) 10th mode.

Figure 6.- Comparison of experimental and analytical nodal patterns of TDNiCr panel.

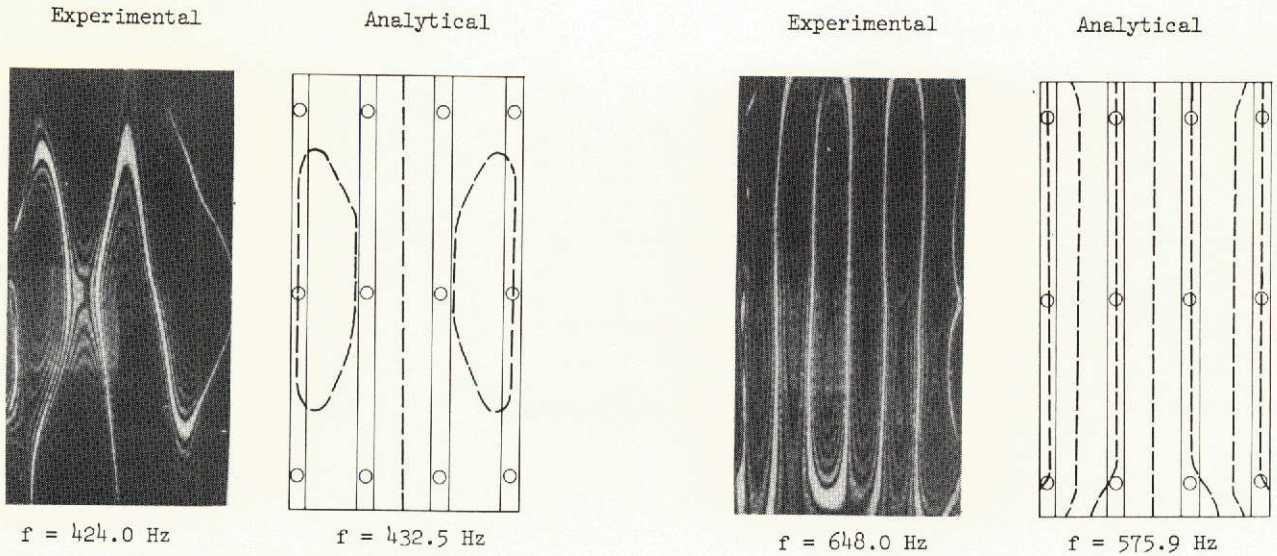

(e) 18th mode.

(f) 29th mode.

(g) 36th mode.

(h) 40th mode.

L-74-1039

Figure 6.- Concluded.

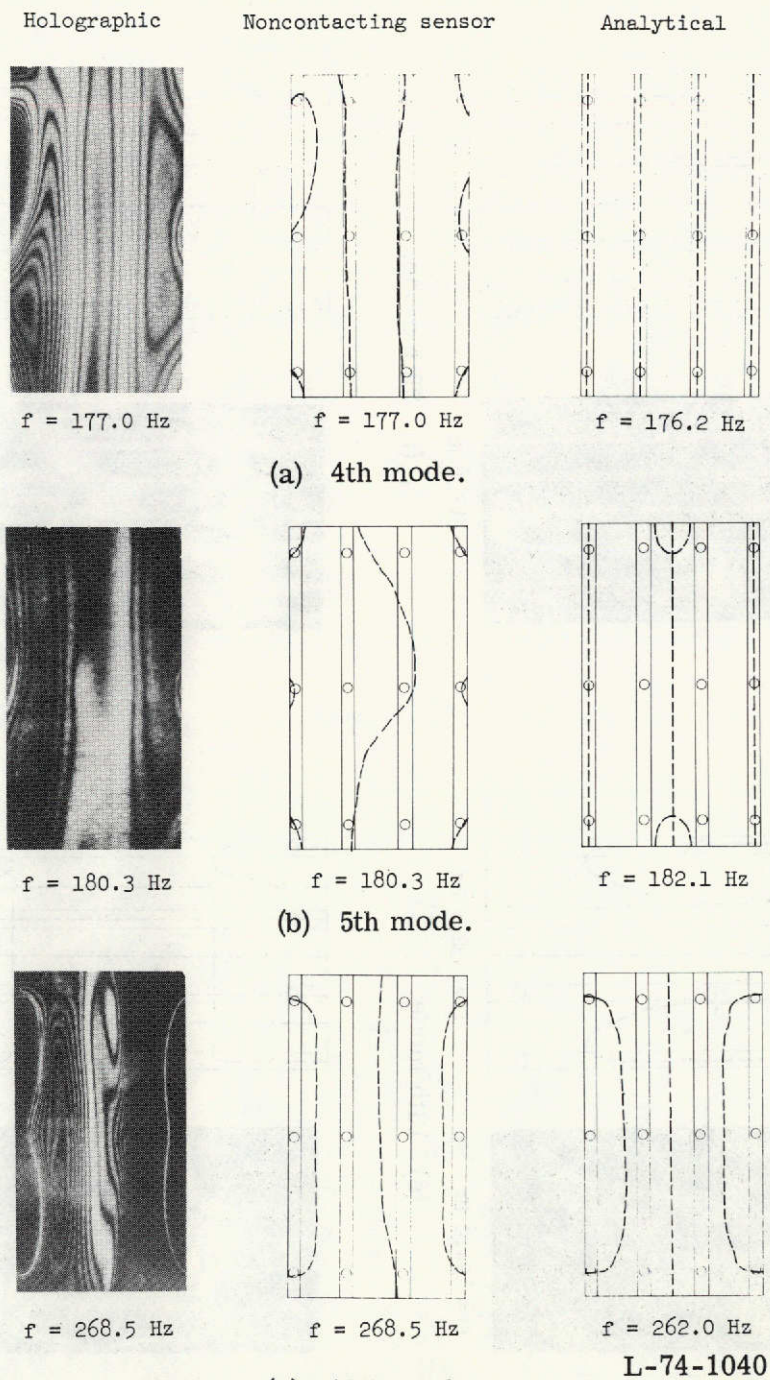

Figure 7.- Comparison of nodal patterns determined with noncontacting proximity sensor and holographic technique.

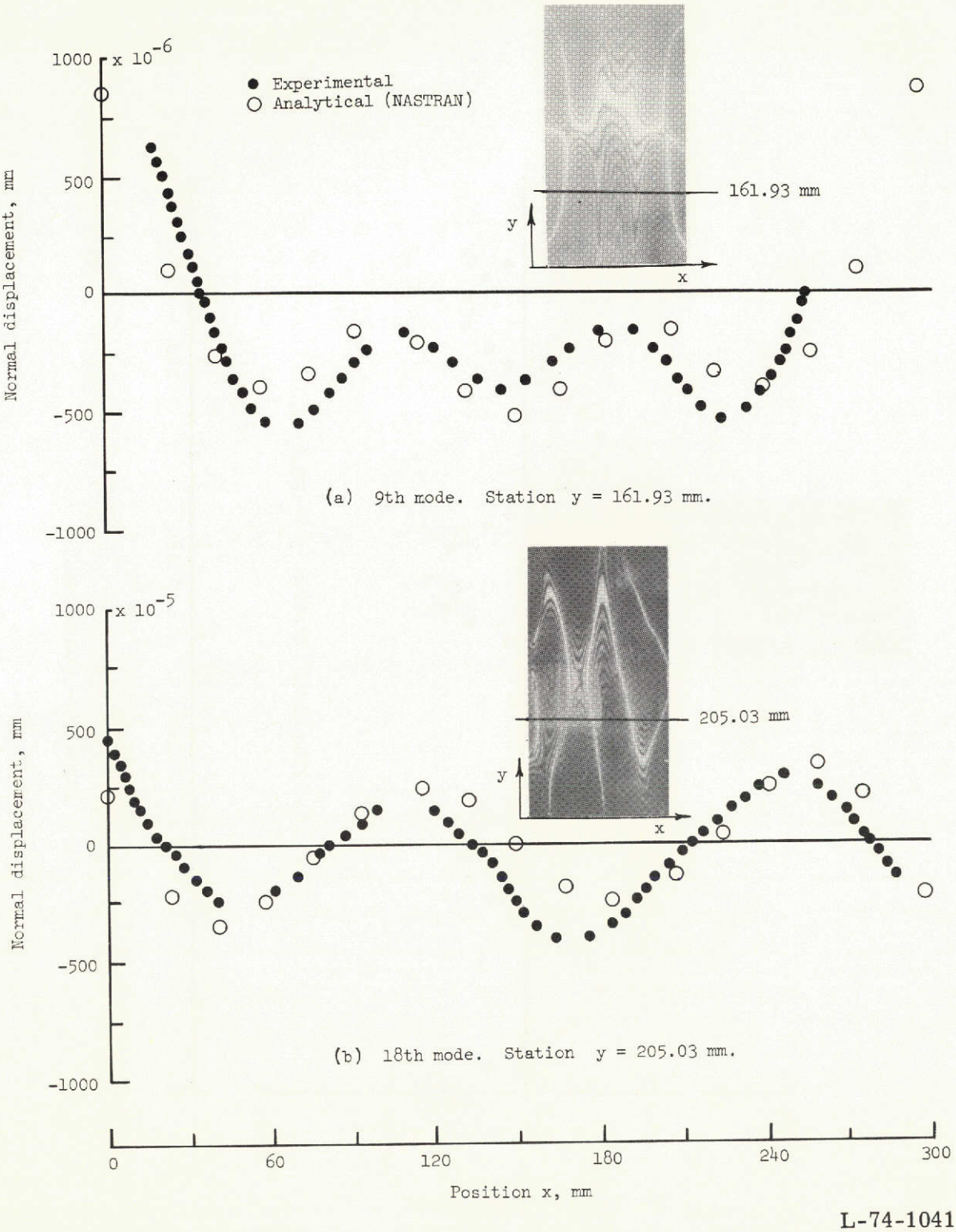

L-74-1041

Figure 8.- Comparison of experimental and analytical modal displacements.

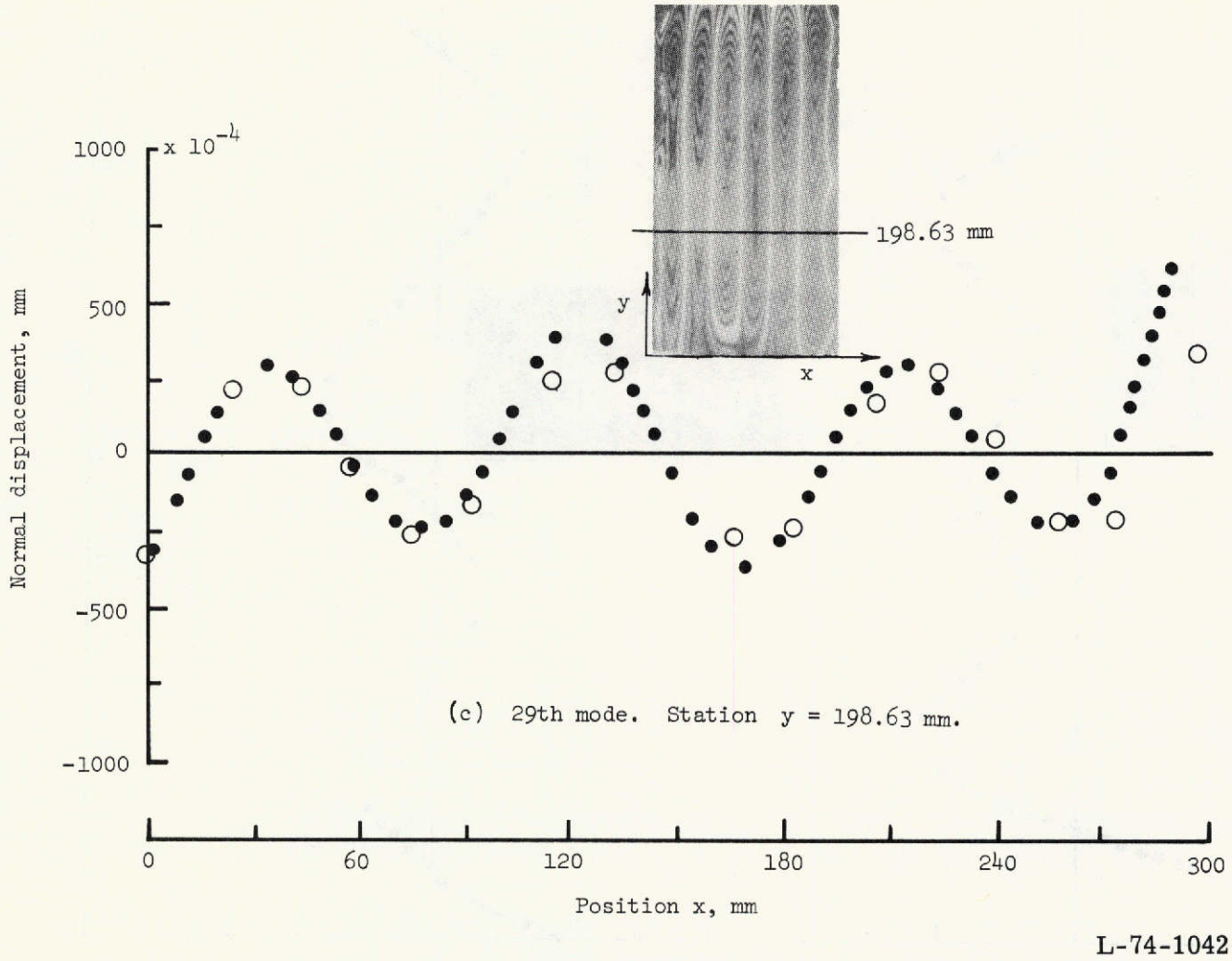

Figure 8.- Concluded.